PHYSICAL REVIEW E **75**, 065401(R) (2007)

Direct evidence of strongly inhomogeneous energy deposition in target heating with laser-produced ion beams

E. Brambrink,[1,*] T. Schlegel,[2] G. Malka,[3] K. U. Amthor,[4] M. M. Aléonard,[3] G. Claverie,[3] M. Gerbaux,[3] F. Gobet,[3] F. Hannachi,[3] V. Méot,[5] P. Morel,[5] P. Nicolai,[6] J. N. Scheurer,[3] M. Tarisien,[3] V. Tikhonchuk,[6] and P. Audebert[1]

[1]*Laboratoire pour l'Utilisation des Lasers Intenses (LULI), Unité Mixte No. 7605 CNRS–CEA–Ecole Polytechnique–Université Pierre et Marie Curie, Palaiseau, France*

[2]*Gesellschaft für Schwerionenforschung, Darmstadt, Germany*

[3]*Centre d'Etudes Nucléaires de Bordeaux-Gradignan, 33175 Gradignan, France*

[4]*Institut für Optik und Quantenelektronik, Friedrich-Schiller-Universität Jena, Germany*

[5]*CEA/DAM, Ile de France, Boîte Postale 12, 91680 Bruyères-le-Châtel, France*

[6]*CELIA, Université Bordeaux 1, 33175 Gradignan, France*

(Received 4 April 2006; revised manuscript received 20 March 2007; published 6 June 2007)

We report on strong nonuniformities in target heating with intense, laser-produced proton beams. The observed inhomogeneity in energy deposition can strongly perturb equation of state (EOS) measurements with laser-accelerated ions which are planned in several laboratories. Interferometric measurements of the target expansion show different expansion velocities on the front and rear surfaces, indicating a strong difference in local temperature. The nonuniformity indicates at an additional heating mechanism, which seems to originate from electrons in the keV range.

DOI: 10.1103/PhysRevE.75.065401 PACS number(s): 52.50.Gj, 05.70.Ce, 52.38.Ph

The equation of state (EOS) of materials in the warm dense matter regime is of great importance for research in various fields like astrophysics, geophysics, plasma physics, or the related topic of inertial confinement fusion [1]. The EOS in such strongly coupled plasmas is unknown for many materials due to the difficulty of producing samples of matter in the corresponding state. Moreover, neither perturbative plasma theories nor standard solid state models can be applied in this part of the phase diagram.

The appearance of short and intense beams of energetic charged particles or photons promotes new possibilities of target heating up to eV temperatures at sufficiently short times (≈ps), before any remarkable hydrodynamic expansion occurs. The quasi-isochoric heating stage will be followed by an isentropic expansion phase [2]. For an accurate EOS measurement, it is essential to deposit the energy in the target with spatial homogeneity. Heavy-ion beams [3] can provide these requirements in principle, but available accelerators cannot deliver sufficient beam intensity to reach high temperatures at solid density.

A few years ago, laser-accelerated proton beams with huge numbers of particles (up to 10^{13}) [4–7] in short bunches (≈ps) [8] and with small diameters (typical initial diameter of the beam 100–200 μm) were developed. The measured low emittance [9] implies an additional opportunity for further focusing to even smaller spot sizes [10]. This heating source of protons will allow EOS measurements in regions of the phase diagram hardly to be reached by other drivers [11] (warm dense matter).

A major issue for the heating scheme with laser-accelerated energetic protons is the homogeneity of their energy deposition. The Boltzmann-like energy spectrum resulting from laser acceleration always provides a large number of protons, which are stopped inside the target, causing high energy deposition at the end of their trajectory (Bragg peak). The overall energy deposition of these protons is very high, which is desirable for reaching high temperatures, but unfortunately introduces also some inhomogeneity in the temperature distribution, which is problematic for an accurate EOS measurement.

In this Rapid Communication we report on strong deviations from homogeneous heating of targets, which were irradiated by laser-generated proton beams. The nonuniformity in the plasma expansion was detected by means of interferometry. We will discuss possible mechanisms that could be responsible for the observed phenomenon.

The experiment was performed at the 100 TW laser system of the Laboratoire pour l'Utilisation des Lasers Intenses (LULI). A laser beam with 20 J energy in 300 fs was focused with an $f/4$ off-axis parabola onto a 13-μm-thick aluminum foil providing peak intensities of $(2-5)\times 10^{19}$ W/cm^2 to generate a proton beam. At a distance of 300 μm behind the primary interaction target we placed a 10-μm-thick plastic foil, which was irradiated by the proton beam.

The experimental setup, typical for isochoric heating of matter with laser-produced proton beams, is sketched in Fig. 1. Two thin foils are placed at a small distance from each other; the first one is illuminated by an intense laser beam. The protons, emitted from the rear surface of this target, hit the second foil and deposit some energy in it. To keep the proton density as high as possible, the distance between the two targets must be small.

The expanding foils were probed by a subpicosecond frequency-doubled (532 nm) laser beam, propagating parallel to both target surfaces. This probe beam was split to obtain an interference pattern and an optical shadowgram. In both diagnostics, the target was imaged with a magnification of $\times 10$; the spatial resolution was better than 5 μm. The delay between the main laser and the probe beam was measured with a streak camera, providing an uncertainty between the two beams of ±10 ps.

*erik.brambrink@polytechnique.fr

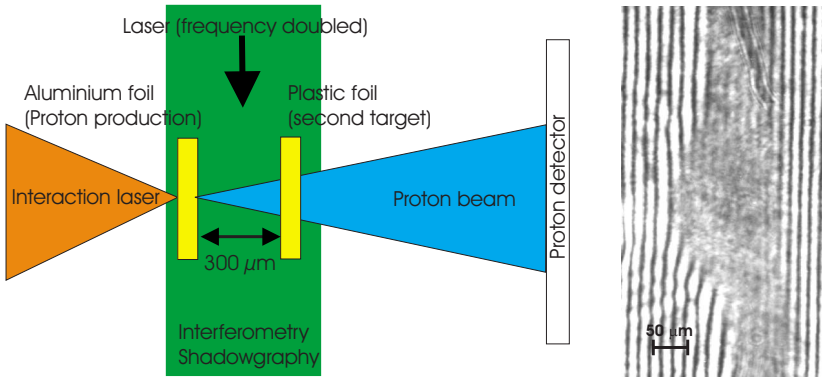

FIG. 1. (Color online) Experimental setup. Laser-generated protons heat a second foil placed 300 μm away from the primary target. The plasma expansion is measured by interferometry. The right side shows an interferogram of the second foil 480 ps after the onset of the laser pulse.

The proton beam was monitored by a stack of radio chromic film (RCF) [12] and (p,n) nuclear reactions in copper samples, which allow evaluation of the energy deposited in the second foil by the fast protons.

By varying the delay between the main interaction beam and the probe beam, the plasma expansion was measured at distinct times to study its temporal evolution. The interferograms were deconvoluted with an Abel inversion to calculate the radial density profile from the fringe shifts. Due to the steep gradient, this was possible only in a limited region of the plasma. From the shadowgraphs, we obtained the position of the critical surface for the probe laser light as a function of time.

Figure 1 (right side) shows an interferometric image of the proton-heated foil (secondary target) 480 ps after the interaction of the main pulse with the primary target. The difference between the front and rear side expansion is obvious. At this time no expansion on the rear surface is visible, while on the front side an extended plasma gradient has already built up. This observation indicates a much higher temperature on the front surface than on the rear one.

To infer the corresponding plasma parameters, responsible for this behavior, we performed simulations with the hydrodynamic code MULTI (which treats electronic and radiative heat transport) [13], using table from the SESAME database [14] for the equation of state. By varying the initial parameters of the expanding foil, we were able to reproduce the experimental results.

Figure 2 (left) shows the electron density profile along the symmetry axis (identical with laser and proton beam axes) 387 ps after the onset of the laser pulse. The plasma has a scale length (drop of density by a factor $1/e$) of 16 μm and the maximum resolvable electron density was $\approx 10^{20}/\mathrm{cm}^3$. The same figure shows the electron density profile deduced from a hydrodynamic simulation, assuming an 80-nm-thick layer with an initial temperature of 70 eV. It contains also simulation results varying both the temperature and the thickness of the heated layer.

The uncertainty on the initial position of the target surface (≈ 15 μm) results in a limited precision for the thickness of the heated layer, which can therefore vary between 50 and 200 nm in the present case. The temperature depends mainly on the gradient. Consequently, this value is much more precise (± 10 eV).

In Fig. 2 (right), the position of the shadow of the expanding plasma, which is determined by the diffraction of the light in the plasma gradient and corresponds in that specific case to a density of $\approx 10^{20}$ cm^{-3}, is plotted with respect to the initial position of the target surface as a function of time. The time $t=0$ corresponds to the time when the laser hits the proton production target. In the studied time domain, we find a nearly constant expansion velocity of 2.1×10^5 m/s. The expansion seems to develop instantaneously, within the resolution of the diagnostic method, starting with the strike of the laser on the primary target.

We compared these results with the plasma expansion obtained from the simulations with the parameters mentioned above. The line in Fig. 2 (right) shows the calculated position of the critical surface as a function of time. A good agreement is observed between the experimental and simulation data.

The transverse dimension of the plasma is around 150 μm, which corresponds quite well to the calculated beam size of the energetic protons on the entrance surface of the secondary target [15].

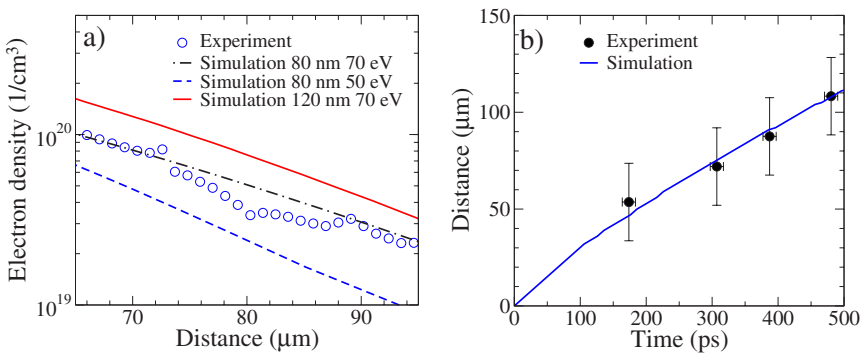

FIG. 2. (Color online) Electron density profile after 387 ps and expansion deduced from the shadowgraphs. Both experimental results were well reproduced by hydrodynamic simulations assuming an 80-nm-thick hot layer on the front surface.

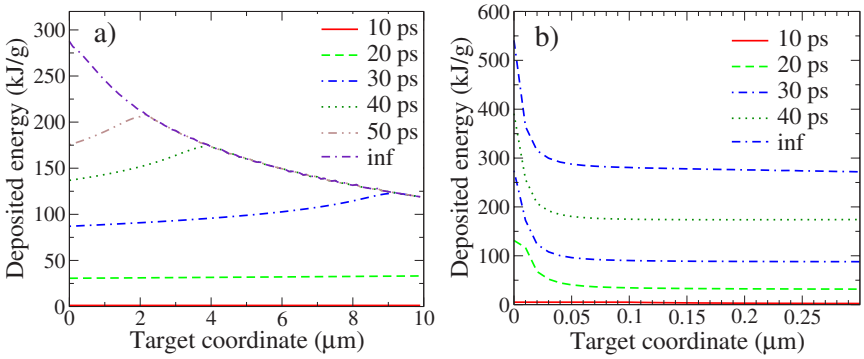

FIG. 3. (Color online) Energy deposition in the foil assuming heating either (a) by protons only or (b) by protons and comoving electrons.

From the rear surface of this target no expansion was visible up to 500 ps. It did not make sense to probe at later times, because the plasma, expanding from the primary target, starts to collide with the secondary foil. For the expansion at this time we can give an upper limit of 30 μm, because a very small expansion could be covered by the edge of the target. We would arrive at the same value when simulating the foil expansion at temperatures of some eV.

The heating of solid targets with laser-generated protons is expected to be inhomogeneous *ab initio* due to the Boltzmann-like energy distribution of the fast protons and the nonlinearity of the stopping process itself. Nevertheless, the hot surface layer observed in the experiment cannot be explained by proton heating only. Protons, being slow enough to deposit their energy only in the first micrometer, would arrive much later in time and would cause a corresponding delay in the expansion of the front surface ($>$50 ps), which was not observed.

To illustrate this process, we calculated the energy deposition by laser-generated protons, using SRIM stopping power tables [16]. The RCF diagnostics delivered an exponential spectrum of 5×10^{11} protons with a mean energy of $\approx$3 MeV and a maximum energy of 15 MeV, which is comparable to the results of the nuclear activation method. The latter will be published elsewhere. The low-energy spectrum, which cannot be detected with the RCF stack, was taken from previous experiments [17] under similar laser and target conditions. The results are shown in Fig. 3(a): the beam enters a 10-μm-thick plastic foil from the left (zero target coordinate).

At the beginning ($<$20ps), the heating is homogeneous; protons arriving up to this time are not stopped inside the target. After 30 ps protons with a mean free path of the order of the target thickness arrive and will be stopped in the back of the foil. The higher stopping power at the end of the range (Bragg Peak) leads to a higher temperature on the rear target surface. At later times, with decreasing proton energy, this peak is drifting toward the front surface of the target. As the number of protons is increasing with decreasing energy, the overall energy deposited in the front layers of the target is much higher than that on the rear side. Nevertheless, the calculated difference (a factor of 2 between front and back) is lower than the measured one and appears later in time (after 50 ps). Consequently, there must be an additional heating mechanism present. Our experiment suggests that this process is (a) quasi-instantaneous (the second target is heated within the first 30 ps after the laser has hit the first target); (b) short range (less than the first micrometer is heated only); intense (according to the EOS around 7800 kJ/g are needed to heat up to the proposed temperature); and (d) heating a radial zone with $\approx$150 μm diameter.

We have shown above that pure proton heating can be excluded, although the transverse dimensions of the proton beam and the heated zone fit quite well. Other ion species have typically a low occurrence under such experimental conditions. In addition, they will arrive too late, like the low-energy protons. Radiative heating is one option, especially since it does not oppose the temporal characteristics of the observed feature. The laser-irradiated target, which will be the radiation source in our case, has a temperature of around 180 eV, as we deduced from the interferometry. A detailed study will be published elsewhere. This heating source will cause an energy deposition of about 150 kJ/g in the surface layer of the secondary foil, following calculations with a view factor hydrocode [18]. In addition, the simulations show that the transverse dimension and the thickness of the heated zone would be much larger than experimentally observed. Finally, the high-energy electrons ($E\geqslant$MeV), coming from the first target, are not numerous enough to heat the foil to temperatures of tens of eV. They pass through the secondary target with the result of homogeneous but weak heating. An obvious suggestion is energy deposition by electrons with lower energy, comoving with the protons. Isochoric heating by laser-generated fast electrons with similar energies is a well-known effect in laser-target interaction, described first in [19].

The proton beam is assumed to be quasineutral at a large distance from the target, which is one reason for its low emittance [9]. To estimate the effect in the case of a neutral beam, we assume that each proton is accompanied by an electron with the same velocity (charge and current neutralization). Since electrons have a much lower mass (1830 times smaller than protons), they carry a correspondingly smaller energy and have a small penetration depth (submicrometer). Figure 3(b) shows the energy deposition taking into account comoving electrons. We can state that heating by these electrons is essential at early times. The temperature achieved is approximately two times larger than for pure proton heating. However, this effect is yet a factor of 10 too low to fit the observed values. In a more realistic scenario, the influence of such electron heating will be even lower, because the absorbed energy is dissipated to a larger volume

(>100 nm depth) by thermal electrons in a short time. Consequently, the hot surface layer becomes broader and colder. Nevertheless, we have seen that such "cold" comoving electrons will provide fast, inhomogeneous heating, which is stronger than the heating by radiation.

To explain the observed strong heating, an advanced model is necessary. The high-energy protons need only some picoseconds to reach the secondary target and the laser-generated fast electrons do not slow down completely in this short time. Therefore, it is more likely, that the mean velocity of the comoving electrons in this phase of expansion is higher than that of the protons, but they are confined in the first target plasma by the electrostatic field connected with the ion front. When this front hits the second target, the confinement breaks. The hot electrons can now reach the surface of the secondary foil, be finally stopped there, and heat a small layer to the observed temperatures.

From the calculated plasma parameters we are able to estimate the characteristics of the heating electrons. To match the penetration depth of around 80 nm given by the hydrodynamic simulations we need an electron energy of several keV. This corresponds quite well to the electron energy expected due to adiabatic cooling during the expansion [20]. The heated mass is approximately 1.5 ng. For the specific energy deposition mentioned above, we need 10 mJ electron energy to heat the sample. This corresponds to $\approx 3 \times 10^{13}$ electrons stopped in the secondary target. With simple estimations (30% conversion of laser energy in the focal spot to hot electrons [21], mean electron energy of 2 MeV [22]), we arrive at a number of 1.6×10^{13} electrons for the present laser parameters. This value is comparable to the required number that we deduced from our estimations. Finally, the electrons would reach the secondary target with the most energetic protons in less than 15 ps, which is fast enough for the reported heating.

We demonstrated observations of a strong inhomogeneous energy deposition by laser-produced proton beams. The temperature on the front surface of the heated target, deduced from expansion measurements, was of the order of 70 eV and therefore much higher than expected after energy deposition by protons only. The instantaneous heating points at a mechanism associated with comoving fast electrons. From the achieved foil surface temperature we conclude the electron energies are in the keV regime.

A detailed modeling of the energy deposition and the temperature distribution in the secondary target needs more information about the electron spectrum. The initial energy distribution of fast electrons propagating through the laser-irradiated target could not be measured. However, from particle-in-cell simulations we know that it can be described by a two-temperature distribution [23]. This spectrum will be modified during electron transport in the first target as well as in between both targets by self-generated electric and magnetic fields. Further theoretical investigations are necessary to understand the underlying processes in detail.

The results of this Rapid Communication have particular influence on recent experiments exploring the equation of state of a sample irradiated with laser-produced protons. Since the details of the energy deposition mechanism remain partly unexplored, care has to be taken in the interpretation of these measurements. Although the strongest heating seems to be restricted to a thin surface layer (<1 μm), a small influence on the bulk of the target cannot be excluded. One could try to suppress this additional heating, deflecting the keV electrons with the help of a magnetic field. On the other hand, the additional heating mechanism discovered opens possibilities for a better understanding of the particle acceleration processes and improved schemes for isochoric heating.

We thank the staff of the LULI laser for their ongoing help during the experiment. This work was supported by Grant No. E1127 from Région Ile-de-France and a grant from Région Aquitaine.

[1] http://www.sc.doe.gov/henp/np/program/docs/HEDP-Report.pdf
[2] Ya. Z. Zeldovich and Yu. P. Raizer, *Physics of Shock Waves and High-Temperature Hydrodynamic Phenomena* (Academic Press, London, 1967).
[3] D. H. H. Hoffmann *et al.*, Phys. Plasmas **9**, 3651 (2002); N. A. Tahir *et al.*, Phys. Rev. Lett. **95**, 035001 (2005).
[4] S. P. Hatchett *et al.*, Phys. Plasmas **7**, 2076 (2000).
[5] E. L. Clark *et al.*, Phys. Rev. Lett. **84**, 670 (2000).
[6] A. Maksimchuk, S. Gu, K. Flippo, D. Umstadter, and V. Y. Bychenkov, Phys. Rev. Lett. **84**, 4108 (2000).
[7] Y. Murakami *et al.*, Phys. Plasmas **8**, 4138 (2001).
[8] L. Romagnani *et al.*, Phys. Rev. Lett. **95**, 195001 (2005).
[9] T. E. Cowan *et al.*, Phys. Rev. Lett. **92**, 204801 (2004).
[10] P. K. Patel *et al.*, Phys. Rev. Lett. **91**, 125004 (2003).
[11] M. E. Foord, D. B. Reismann, and P. T. Springer, Rev. Sci. Instrum. **75**, 2586 (2004).
[12] W. L. McLaughlin *et al.*, Nucl. Instrum. Methods Phys. Res. A **320**, 165 (1991).
[13] R. Ramis, R. Schmalz, and J. Meyer-ter-Vehn, Comput. Phys. Commun. **49**, 475 (1988).
[14] Los Alamos National Laboratory Report No. La-Ur-92-3407, edited by S. P. Lyon and J. D. Johnson (Group T-1, 1992).
[15] E. Brambrink *et al.*, in Proceedings of the Europhysics Conference 2005 (Europhysics Conference Abstracts, Vol. 29C, 2005), http://eps2005.ciemat.es/papers/start.htm
[16] J. Ziegler, http://www.srim.org
[17] M. Cuneo (private communication).
[18] T. Schlegel *et al.* (to be published).
[19] A. Saemann *et al.*, Phys. Rev. Lett. **82**, 4843 (1999).
[20] P. Mora, Phys. Rev. E **72**, 056401 (2005).
[21] M. H. Key *et al.*, Phys. Plasmas **5**, 1966 (1998).
[22] S. C. Wilks, W. L. Kruer, M. Tabak, and A. B. Langdon, Phys. Rev. Lett. **69**, 1383 (1992).
[23] Q. L. Dong, J. Zhang, and H. Teng, Phys. Rev. E **64**, 026411 (2001).